PHYSICAL REVIEW LETTERS

Superconducting Fe-Based Compounds $(A_{1-x}Sr_x)Fe_2As_2$ with $A=$ K and Cs with Transition Temperatures up to 37 K

Kalyan Sasmal,[1] Bing Lv,[2] Bernd Lorenz,[1] Arnold M. Guloy,[2] Feng Chen,[1] Yu-Yi Xue,[1] and Ching-Wu Chu[1,3,4]

[1]*TCSUH and Department of Physics, University of Houston, Houston, Texas 77204, USA*
[2]*TCSUH and Department of Chemistry, University of Houston, Houston, Texas 77204, USA*
[3]*Lawrence Berkeley National Laboratory, 1 Cyclotron Road, Berkeley, California 94720, USA*
[4]*Hong Kong University of Science and Technology, Hong Kong, China*
(Received 13 June 2008; published 5 September 2008)

New high-T_c Fe-based superconducting compounds, AFe_2As_2 with $A=$ K, Cs, K/Sr, and Cs/Sr, were synthesized. The T_c of KFe_2As_2 and $CsFe_2As_2$ is 3.8 and 2.6 K, respectively, which rises with partial substitution of Sr for K and Cs and peaks at 37 K for 50%–60% Sr substitution, and the compounds enter a spin-density-wave state with increasing electron number (Sr content). The compounds represent p-type analogs of the n-doped rare-earth oxypnictide superconductors. Their electronic and structural behavior demonstrate the crucial role of the (Fe_2As_2) layers in the superconductivity of the Fe-based layered systems, and the special feature of having elemental A layers provides new avenues to superconductivity at higher T_c.

Guided by the rule that high-temperature superconductivity usually occurs in strongly correlated electron layered systems as in the copper oxides [1], Hosono's group started a few years ago to search for superconductivity in quaternary equiatomic rare-earth transition-metal oxypnictides, *ROTPn*, where $R=$ rare earth, $T=$ transition metal, and Pn = pnictogen. Indeed, superconductivity was found in *ROTPn*, where $R=$ La, $T=$ Ni and Fe, Pn = P and As, with transition temperatures (T_c) up to 26 K in F-doped $LaOFeAs$ [2]. The observation generated immense excitement due to the high T_c and the significantly large amount of a magnetic component, Fe, which is considered antithetic to conventional s-wave superconductivity. In the ensuing few weeks after the initial report of $T_c=26$ K in La(O,F)FeAs, the T_c was quickly raised to 41–52 K in other F-doped samples, R(O, F)FeAs, replacing La with other trivalent R with smaller ionic radii [2–7]. This is consistent with the reported positive pressure effect on the T_c of La(O,F)FeAs [8]. Thus, a new class of materials with a promising potential for high T_c that may rival the well-known cuprate high-temperature superconductors was born. Intensive studies followed to further raise their T_c and to unravel the underlying mechanism for superconductivity in R(O, F)FeAs. A subsequent high pressure study shows that the pressure effect on the T_c of Sm(O,F)FeAs depends on F doping, i.e., positive when the sample is underdoped but negative when overdoped, similar to the cuprates [9]. The results suggest that the maximum T_c of R(O, F)FeAs is around $\sim$55 K and that higher T_c's ($>$55 K) may yet be discovered in compounds that are chemically different but physically related to R(O, F)FeAs. We therefore examined the structurally related layered system AFe_2As_2, with $A=$ K, Cs, Sr, (K/Sr), or (Cs/Sr). We found KFe_2As_2 and $CsFe_2As_2$ exhibit superconducting transitions at 3.8 and 2.6 K, respectively. Furthermore,

with Sr substitution, the T_c of $(K_{1-x}Sr_x)Fe_2As_2$ and $(Cs_{1-x}Sr_x)Fe_2As_2$ increases to a maximum T_c of 36.5 and 37.2 K, respectively, at $x\sim0.5$–0.6. A new family of Fe-based layered compounds with a relatively high T_c is thus discovered. Given that elemental K, Cs, (K/Sr), or (Cs/Sr) layers separate the (Fe_2As_2) layers, this class of superconducting materials may provide new ways to raise T_c.

ROFeAs crystallize in the tetragonal ZrCuSiAs-type structure [2,3] that consists of transition-metal pnictide (Fe_2As_2) layers sandwiched by rare-earth oxide (R_2O_2) layers, as shown in Fig. 1(a). Similar to the cuprate high-temperature superconductors, the charge carriers are supposed to flow within the (Fe_2As_2) layers, and the (R_2O_2)-layers act as "modulation doping" layers while retaining the structural integrity of the (Fe_2As_2) layers. However, details of the layered structure of ROFeAs are different from the high T_c cuprates: the formally divalent Fe is tetrahedrally coordinated to four As atoms, whereas the divalent Cu in cuprates is coordinated to four oxygens in a square planar manner. AFe_2As_2 ($A=$ K and Cs) crystallize in the $ThCr_2Si_2$ structure type [10,11]. It features identical (Fe_2As_2) layers as in ROFeAs, but separated by single elemental A layers, as shown in Fig. 1(b). In stacking the (Fe_2As_2) layers in AFe_2As_2, the layers are oriented such that the As-As distances between adjacent layers are closest. Nevertheless, interlayer As-As distances in AFe_2As_2 are effectively nonbonding. In ROFeAs, adjacent (Fe_2As_2) layers are stacked parallel, with identical orientations, and the (Fe_2As_2) layers are further isolated by more complex (La_2O_2) slabs.

We have undertaken a systematic study of the $(K_{1-x}Sr_x)Fe_2As_2$ for $x=$ 0, 0.1, 0.3, 0.5, 0.6, 0.7, 0.8, 0.9, and 1.0. In addition, representative superconducting phases of $(Cs_{1-x}Sr_x)Fe_2As_2$ with $x=$ 0.5 and 0.6, as well as $CsFe_2As_2$, were studied. All ternary compounds were pre-
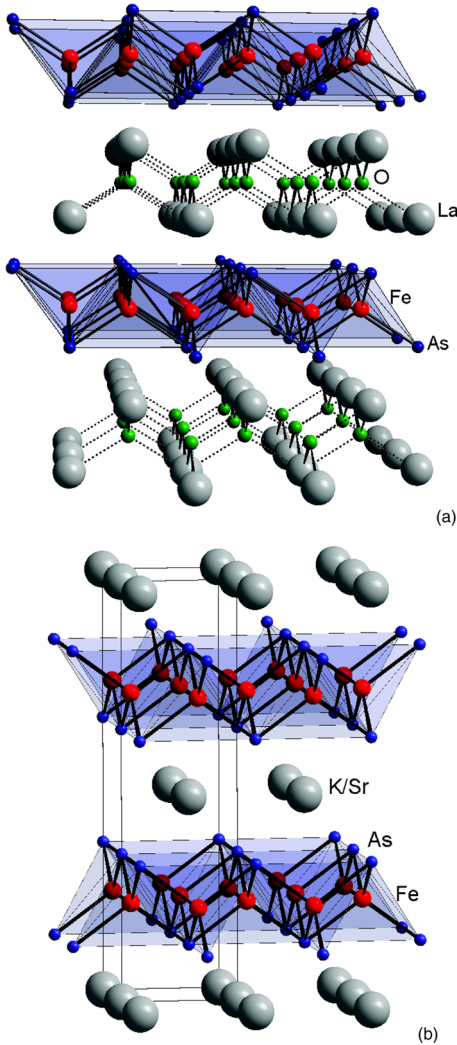
FIG. 1 (color online).   (a) Crystal structure of LaOFeAs;
(b) crystal structure of $(K/Sr)Fe_2As_2$ and $(Cs/Sr)Fe_2As_2$.

pared by high-temperature solid state reactions of high
purity K, Cs, and Sr with FeAs. Phase-pure FeAs powder
was prepared from the reaction of pure elements in sealed
quartz containers at 600–800 °C. Polycrystalline samples
of the title compounds were prepared and handled under
purified Ar atmosphere. Samples were prepared as follows:
stoichiometric amounts of the starting materials were
mixed and pressed into pellets. The pellets were sealed in
welded Nb tubes under Ar. The reaction charges were
jacketed within sealed quartz containers, and then heated
for 20–24 h at 1000, 950, and 700 °C for $SrFe_2As_2$,
KFe_2As_2, and $CsFe_2As_2$, respectively. In addition,
$SrFe_2As_2$ was preheated at 1200 °C for 1.5 h, and
$CsFe_2As_2$ was preheated at 550 °C for 12 h. For the
mixed-metal samples, $(K, Sr)Fe_2As_2$ and $(Cs, Sr)Fe_2As_2$,
stoichiometric amounts of the ternary iron arsenides were
thoroughly mixed, pressed and then annealed within
welded Nb containers (jacketed in quartz) at 900 °C for
20–30 h. The $SrFe_2As_2$ and the mixed-metal, (K-Sr) and
(Cs-Sr), compounds are stable to air and moisture.

However, KFe_2As_2 and $CsFe_2As_2$ are air and moisture
sensitive. The resulting polycrystalline samples were in-
vestigated by powder x-ray diffraction. X-ray diffraction
data of the end compounds (i.e., $x = 0.0$ and 1.0), shown in
Fig. 2, can be completely indexed to the tetragonal
$ThCr_2Si_2$ structure. The refined tetragonal cell parameters
of the isostructural mixed-metal phases show a trend in cell
volume that agrees with the atomic radii of the metals; i.e.,
cell volumes increase with increasing alkali metal content.
In addition, the c/a ratios changes significantly with Sr
incorporation in that the ratio decreases with increasing Sr
content, while the a parameter nearly remains unchanged.
The contraction in the c/a ratio is most significant in the
Cs compounds. This implies that the interlayer distance
between the (Fe_2As_2) layers and the relevant As-As dis-
tances decrease with Sr content. $\varrho(T)$ was measured by
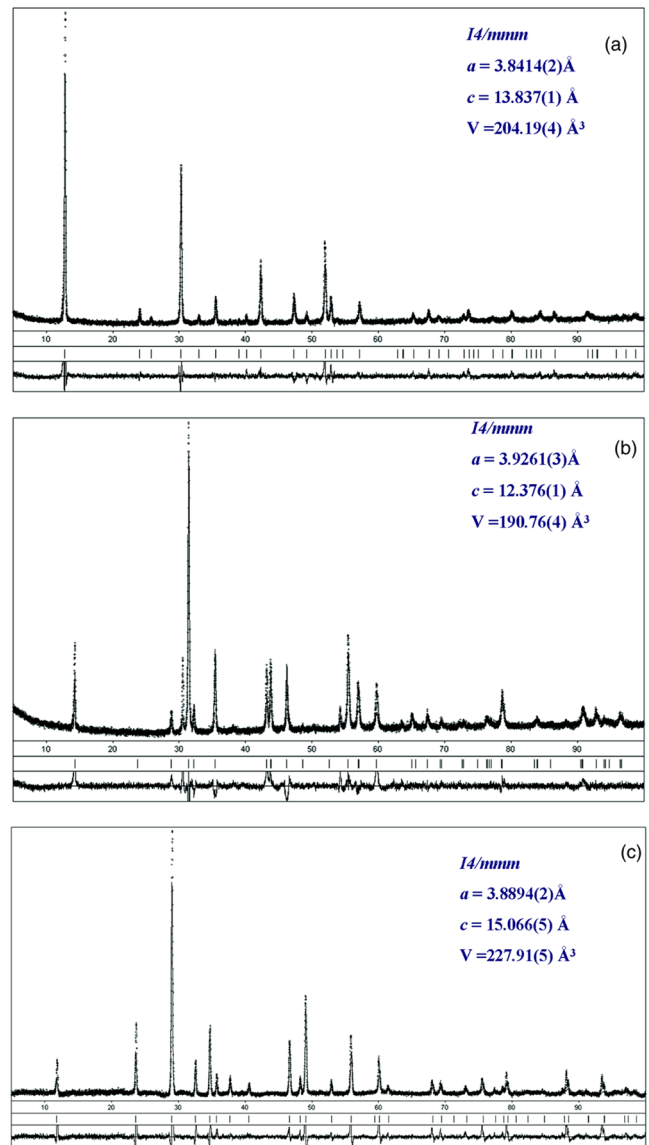employing a standard 4-probe method using a Linear

FIG. 2 (color online).   (a) Powder diffraction data/Rietveld
refinement: (a) KFe_2As_2, (b) $SrFe_2As_2$, (c) $CsFe_2As_2$.

Research LR-700 ac bridge operated at 19 Hz, and the magnetic field effect on ϱ was measured using a Quantum Design physical property measurement system for temperatures down to 1.8 K and magnetic fields up to 7 T. The temperature dependence of the dc-magnetic susceptibility $\chi(T)$ was measured using Quantum Design SQUID magnetometer at fields up to 5 T. The Seebeck coefficient was measured using a very low frequency ac two-heater method [12].

The resistivities $\varrho(T)$, as a function of temperature and magnetic field, magnetic susceptibilities $\chi(T)$, as a function of temperature, and Seebeck coefficients of the title compounds were measured. The $\varrho(T)$'s of all samples investigated exhibit metallic behavior. Figure 3(a) shows that the ϱ of $SrFe_2As_2$ decreases from room temperature and undergoes a rapid drop at ~ 200 K, indicative of the onset of a spin-density-wave (SDW) state, similar to the isoelectronic $BaFe_2As_2$ [13,14]. The observed noise near room temperature is associated with the condensation of moisture in the samples. Figure 3(a) also shows ϱ of KFe_2As_2 decreasing with temperature, but with a strong

negative curvature, suggesting strong electron-electron correlation. The ϱ finally drops to zero below ~ 3.8 K, indicating a transition to the superconducting state [Fig. 3(a), inset].

All samples, except $SrFe_2As_2$ and $K_{0.1}Sr_{0.9}Fe_2As_2$, display bulk superconductivity as evidenced by the drastic drop of ϱ to zero and a large Meissner effect at T_c. The $\chi(T)$'s for KFe_2As_2 and $CsFe_2As_2$ show superconducting transitions at ~ 3.8 K and ~ 2.6 K as shown in Fig. 4(a) (inset), respectively. The $\chi(T)$ of the samples with highest T_c, $(K_{0.4}Sr_{0.6})Fe_2As_2$ and $(Cs_{0.4}Sr_{0.6})Fe_2As_2$, are also shown in Fig. 4(a). As expected, the magnetic field is observed to suppress the superconducting transitions of $(K_{0.4}Sr_{0.6})Fe_2As_2$ and $(Cs_{0.4}Sr_{0.6})Fe_2As_2$, as shown in Fig. 3(b). Using the Ginzburg-Landau formula on Figs. 3(b) and 3(c), and defining T_c as the temperature at which ϱ drops by 50%, a high $H_{c2}(0)$ of 140 and 190 T can be deduced for $(Cs_{0.4}Sr_{0.6})Fe_2As_2$ and $(K_{0.4}Sr_{0.6})Fe_2As_2$, respectively. Even at the 90% resistivity drop the extrapolated $H_{c2}(0)$ is still high, 110 T for $(Cs_{0.4}Sr_{0.6})Fe_2As_2$ and 153 T for $(K_{0.4}Sr_{0.6})Fe_2As_2$. It is remarkable that these values exceed the critical fields of the fluorine-doped
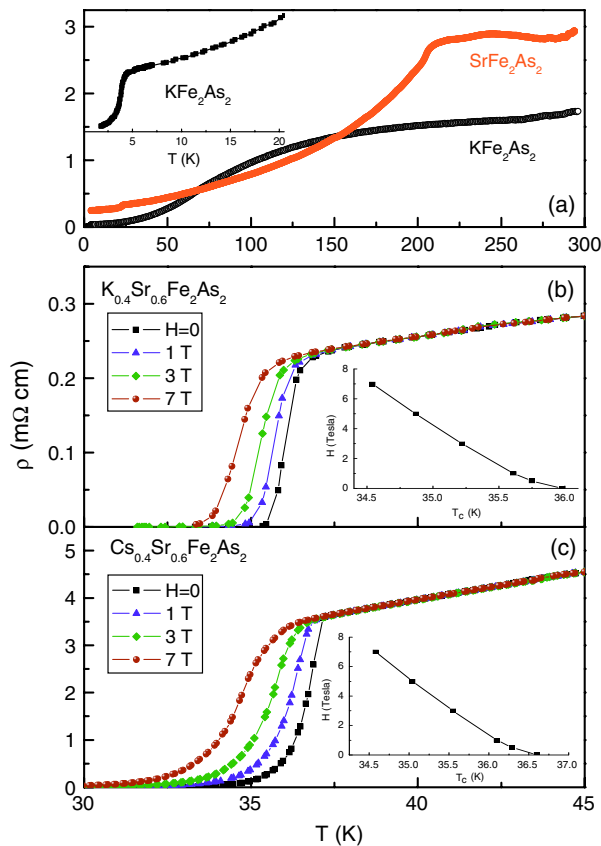

FIG. 3 (color online).   (a) Resistivity of the two end members, $SrFe_2As_2$ and KFe_2As_2. The inset shows the superconducting transition of KFe_2As_2 on an enlarged scale; (b) resistivity at different fields of $K_{0.4}Sr_{0.6}Fe_2As_2$; (c) resistivity at different fields of $Cs_{0.4}Sr_{0.6}Fe_2As_2$. The insets in (b) and (c) show the T dependence of the critical fields as determined from the midpoint of the resistivity drop.
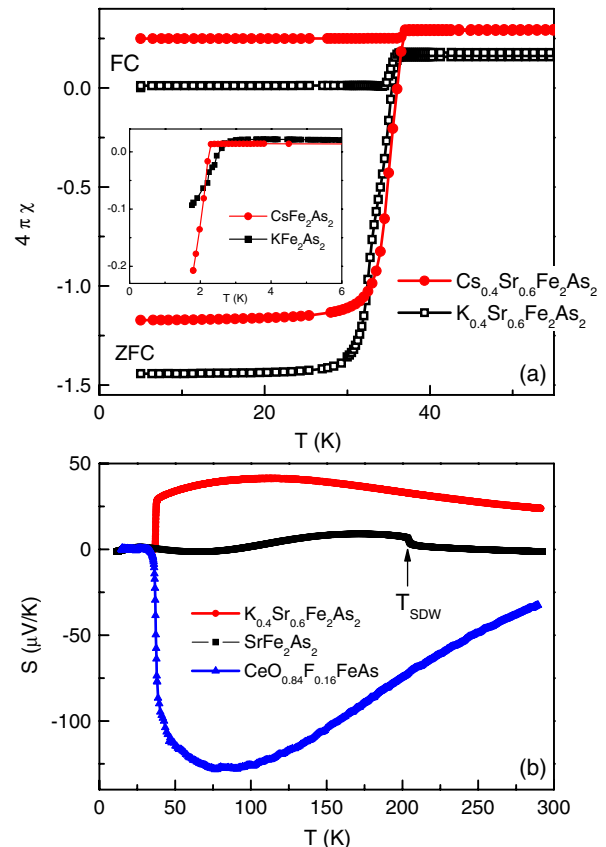

FIG. 4 (color online).   (a) Field cooled (FC) and zero field cooled (ZFC) magnetic susceptibilities of $K_{0.4}Sr_{0.6}Fe_2As_2$ and $Cs_{0.4}Sr_{0.6}Fe_2As_2$ measured at 10 Oe. The inset shows the magnetic susceptibilities of KFe_2As_2 and $CsFe_2As_2$ near T_c; (b) Seebeck coefficients of $K_{0.4}Sr_{0.6}Fe_2As_2$ (top curve), $SrFe_2As_2$ (middle curve), and $CeO_{0.84}F_{0.16}FeAs$ (bottom curve).
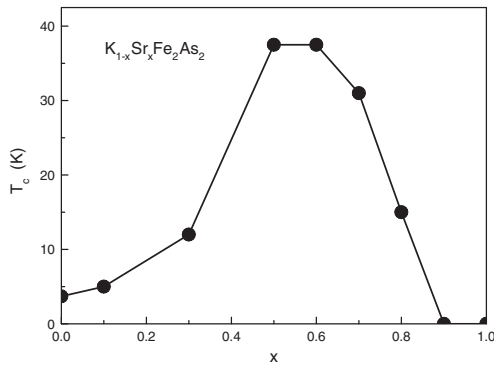
FIG. 5.   Superconducting phase diagram of $K_{1-x}Sr_xFe_2As_2$.

LaOFeAs compound [15]. The superconducting and the SDW transitions, evident from the $\varrho(T)$ and $\chi(T)$, is further confirmed by the measured Seebeck coefficients presented in Fig. 4(b). The significant positive thermoelectric power of $(K_{0.4}Sr_{0.6})Fe_2As_2$ indicates the major carriers in this system are holelike (p type), in contrast to the electronlike large negative thermoelectric power in the superconducting $CeO_{0.84}F_{0.16}FeAs$.

The results of $\varrho(T)$ and $\chi(T)$ for phases with varying Sr content can be summarized by a phase diagram of T_c vs Sr content (x), constructed for $(K_{1-x}Sr_x)Fe_2As_2$, in Fig. 5. A similar phase diagram for $(Cs_{1-x}Sr_x)Fe_2As_2$ is also observed. The diagram shows that the T_c's of KFe_2As_2 and $CsFe_2As_2$ are enhanced continuously by Sr doping and peak at ~ 37 K for Sr substitution levels of 50%–60%. In view of the valence counts of $[(K)^{1+}]_{0.5}(FeAs)^{0.5-}$ in KFe_2As_2 and $[(Sr)^{2+}]_{0.5}(FeAs)^{1-}$ compared to $(RO)^{1+} \times (FeAs)^{1-}$ in $ROFeAs$, KFe_2As_2 exhibits significant electron deficiency, whereas $SrFe_2As_2$ is isoelectronic to $ROFeAs$. Partial substitution of K by Sr corresponds to electron counts approaching the electron count of $ROFeAs$, and the T_c crests at doping levels corresponding to $(FeAs)^{(0.75-0.8)-}$. In contrast, the formal electron count corresponding to the superconducting phase, $RO_{1-x}F_xFeAs$ ($x = 0.15$–0.20), is $(FeAs)^{(1.15-1.20)-}$. Therefore, we conclude that the superconductivity in the (Fe_2As_2) layers almost symmetrically peaks at two different types of carrier densities: p type in $(K/Cs, Sr)Fe_2As_2$, and n type in $R(O, F)FeAs$. These observations demonstrate that Cooper pairs in the Fe_2As_2 layers can be formed by both holes and electrons, similar to the behavior of the high-T_c cuprates. The evolution of superconducting state to a SDW state by electron doping in AFe_2As_2 and the induction of a superconducting state from the SDW state in $ROFeAs$ effectively demonstrates the symmetry in the extended phase diagram (hole and electron carriers) and the unique role of (Fe_2As_2) layers for superconductivity at relatively high temperature. Our results and conclusions prove the significant role of the (Fe_2As_2) layers in superconductivity of the Fe-based layer superconductors, and as the primary cause for nonconventional superconductivity in these compounds. The simple AFe_2As_2 family of compounds also

provides a basis from which T_c may be raised. This may be achieved by constructing more complex homologues of the layered Fe pnictides, similar to what has been carried out in the high-T_c cuprates.

Note added in proof.—After completion of this work we became aware of the work by Rotter, Tegel, and Johrendt [16], reporting the observation of superconductivity in the related compound $K_{0.4}Ba_{0.6}Fe_2As_2$.

[1] See, for example, C. W. Chu, in *Emerging Materials*, Handbook of Superconducting Materials Vol. 2, edited by D. Cardwell and D. Ginley (IOP, Bristol, 2003), Chap. 5.

[2] Y. Kamihara, T. Watanabe, M. Hirano, and H. Hosono, J. Am. Chem. Soc. **130**, 3296 (2008).

[3] H. Takahashi, K. Igawa, K. Arii, Y. Kamihara, M. Hirano, and H. Hosono, Nature (London) **453**, 376 (2008).

[4] X. H. Chen, T. Wu, G. Wu, R. H. Liu, H. Chen, and D. F. Fang, Nature (London) **453**, 761 (2008).

[5] G. F. Chen, Z. Li, D. Wu, G. Li, W. Z. Hu, J. Dong, P. Zheng, J. L. Luo, and N. L. Wang, Phys. Rev. Lett. **100**, 247002 (2008).

[6] Z. A. Ren, J. Yang, W. Lu, W. Yi, G. C. Che, X. L. Dong, L. L. Sun, and Z. X. Zhao, Mater. Res. Innovations **12**, 1 (2008).

[7] Z. A. Ren, J. Yang, W. Lu, W. Yi, X. L. Shen, Z. C. Li, G. C. Che, X. L. Dong, L. L. Sun, F. Zhou, and Z. X. Zhao, Europhys. Lett. **82**, 57002 (2008).

[8] W. Lu, J. Yang, X. L. Dong, Z. A. Ren, G. C. Che, and Z. X. Zhao, New J. Phys. **10**, 063026 (2008).

[9] B. Lorenz, K. Sasmal, R. P. Chaudhury, X. H. Chen, R. H. Liu, T. Wu, and C. W. Chu, Phys. Rev. B **78**, 012505 (2008).

[10] S. Rozsa and H. U. Schuster, Z. Naturforsch. B **36**, 1668 (1981).

[11] A. Czybulka, M. Noak, and H.-U. Schuster, Z. Anorg. Allg. Chem. **609**, 122 (1992).

[12] F. Chen, J. C. Cooley, W. L. Hults, and J. L. Smith, Rev. Sci. Instrum. **72**, 4201 (2001).

[13] M. Rotter, M. Tegel, D. Johrendt, I. Schellenberg, W. Hermes, and R. Pöttgen, Phys. Rev. B **78**, 020503(R) (2008).

[14] Near the completion of our work, the observation of a SDW state in pure $SrFe_2As_2$ was reported by C. Krellner, N. Caroca-Canales, A. Jesche, H. Rosner, A. Ormeci, and C. Geibel, arXiv:0806.1043.

[15] F. Hunte, J. Jaroszynski, A. Gurevuch, D. C. Larbalestier, R. Jin, A. S. Sefat, M. A. McGuire, B. C. Sales, D. K. Christen, and D. Mandrus, Nature (London) **453**, 903 (2008).

[16] M. Rotter, M. Tegel, and D. Johrendt, Phys. Rev. Lett. **101**, 107006 (2008).